Water Resour Manage (2011) 25:2035–2059
DOI 10.1007/s11269-011-9793-2

Using MODFLOW and GIS to Assess Changes in Groundwater Dynamics in Response to Water Saving Measures in Irrigation Districts of the Upper Yellow River Basin

Xu Xu · Guanhua Huang · Zhongyi Qu · Luis S. Pereira

Received: 25 June 2010 / Accepted: 7 February 2011 /
Published online: 2 March 2011

Abstract The irrigation districts of the upper Yellow River basin are highly productive agricultural areas of North China. Due to the severe water scarcity, application of water-saving practices at both farm and district levels are required for sustainable agricultural development. An integrated methodology was developed adopting loose coupling of the groundwater flow model MODFLOW with ArcInfo Geographic Information System to assess the impacts of irrigation water-saving practices and groundwater abstraction foreseen for the year of 2020 on the groundwater dynamics of the Jiefangzha Irrigation System (JFIS) in Hetao Irrigation District, upper Yellow River basin. The model was calibrated and validated with datasets of years 2004 and 2005; the model efficiency EF was respectively 0.98 for calibration and 0.99 for validation. Results of the simulation of the groundwater dynamics of the study area

X. Xu · G. Huang
Chinese–Israeli International Center for Research and Training in Agriculture,
China Agricultural University, Beijing 100083, People's Republic of China

X. Xu · G. Huang (✉)
Center for Agricultural Water Research, China Agricultural University, Beijing 100083,
People's Republic of China
e-mail: ghuang@cau.edu.cn

X. Xu
e-mail: xushengwu@cau.edu.cn

Z. Qu
College of Water Conservancy and Civil Engineering, Inner Mongolia Agricultural University,
Hohhot 010018, People's Republic of China
e-mail: quzhongyi68@sohu.com

L. S. Pereira (✉)
CEER—Biosystems Engineering, Institute of Agronomy, Technical University of Lisbon,
Tapada da Ajuda, 1349–017 Lisbon, Portugal
e-mail: lspereira@isa.utl.pt

show that water-saving practices referring to canal lining and upgrading hydraulic structures applied in 60% of the area, and upgraded farm irrigation technology in 50% of the area may consist of a reasonable solution. Their implementation would lead to reduce groundwater evaporation by 43 mm and the total diversions from the Yellow River by 208 mm, i.e. about 20% of present volumes diverted. Most of routines and strategies for model construction may also be used for other regions, especially for irrigation districts in the upper Yellow River basin.

Keywords Groundwater modelling · Groundwater depth · Groundwater evaporation · Irrigation systems improvement · Seepage and percolation · Hetao Irrigation District

1 Introduction

The Yellow River is the second largest river in China. It supplies water for about 130 million people in nine provinces in the Northwest and North China. The Yellow River basin is an area with severe water scarcity, with less than 500 m^3 per capita (Wang et al. 2006). Agricultural irrigation is the main water use in the basin, accounting for 81% of the total water use (Zhu et al. 2003). The headstream of the Yellow River basin is becoming drier due to climate change, e.g., decrease of precipitation during the last half century (Zhao et al. 2008). In addition, increased water abstractions for industrial, domestic and hydro-power uses exacerbate water scarcity in the basin (Liu and Xia 2004). Due to these water scarcity conditions, the middle and low reaches of the river dried up 21 times during 1972–2008, with 226 days of no-flow in 1997 (Liu and Zheng 2004). Forecasted scenarios on water resources allocation and use in the basin point out the need to reduce irrigation water use (Xu et al. 2002; Yu 2006).

Long time excess water diversions from the river and poor irrigation and drainage management practices have caused severe water logging and salinity in the upstream irrigation districts (Wang et al. 1993; Fang and Chen 2001). Since 2000, diverse water-saving measures have been considered and progressively implemented in irrigation districts located in the upper reaches of the Yellow River to improve both water conveyance and farm water use (Cai et al. 2003; Pereira et al. 2003). Measures for improving water conveyance and distribution include lining of canals, upgrading of hydraulic control structures and better canal water delivery management. Measures for improving water use and productivity at farm include upgraded irrigation scheduling, land levelling of irrigated fields, and improved furrowed and flat basin irrigation systems (Deng et al. 2006; Pereira et al. 2007; Gonçalves et al. 2007). Application of those water-saving technologies together with improved drainage are expected to lower the groundwater table depth (GWD) and to reduce groundwater evaporation, thus leading to better controlling water logging and salinity (Hollanders et al. 2005). Additionally, the increase of groundwater abstraction for municipal and industry uses will accelerate the decline of the groundwater table. However, an excessive lowering of GWD may result in negative impacts on the fragile ecological environment due to reduced capillary rise (Ma et al. 2005; Ruan et al. 2008; Xu et al. 2010). According to Ruan et al. (2008), impacts seem to be major when the GWD becomes deeper than 3 m because capillary rise is then highly reduced, thus

affecting the vegetation water uptake and related growth and yield of crops that may require additional irrigation water. It is therefore important to investigate the impact of human activities on the groundwater dynamics, mainly irrigation water-saving practices and the increase of groundwater abstraction. In this study, the Jiefangzha Irrigation System (JFIS) of Hetao Irrigation District (Hetao) is considered as a typical example. It was selected because former studies were performed there and adequate data were available for the current study.

Groundwater flow models are appropriate tools to assess the effect of foreseen future human activities on groundwater dynamics (Mao et al. 2005; Dawoud et al. 2005; Mylopoulos et al. 2007). However, models require good quality data on the physical and hydrogeological settings. The physical ones refer to topography, land use, soils, canals and drainage ditches, climate and crops demand for water. The hydrogeological settings include the aquifer system and boundary conditions, main hydraulic parameters characterizing each aquifer layer, and the dynamics of groundwater levels. All of them vary both in space and time, thus adopting a Geographic Information System (GIS) in association with a model is helpful. Coupling GIS technology with a process-based groundwater model may facilitate hydrogeological and hydrologic system conceptualization and characterization (Hinaman 1993; Kolm 1996; Gogu et al. 2001), thus also a proper adaptation of the groundwater flow model to the area under study (Brodie 1998). Various examples confirm the appropriateness of GIS applications in groundwater hydrology (San Juan and Kolm 1996; Herzog et al. 2003; Jha et al. 2007; Brunner et al. 2008; Li et al. 2008).

Xu et al. (2009) used MODFLOW 2000 (Harbaugh et al. 2000) coupled with GIS to simulate the groundwater dynamics but the approach used was rather insufficient because a single linear depth-groundwater flux relationship was used, which may result in over- or underestimating groundwater evaporation. In addition, the groundwater table is often above the ground surface in the wetlands and lower lands, as evidenced in remote sensing studies by Wu et al. (2008), which was not considered in the MODFLOW codes applied in that study. Therefore, new approaches were developed for the present study and MODFLOW 2000 codes were modified as described in Section 3.1. These improvements represent a step forwards relative to the referred study. This study also differs from the one described by Xu et al. (2010), where the assessment of impacts of water saving measures on the groundwater dynamics was performed with a lumped groundwater balance model developed purposefully to JFIS. Main differences relative to that study, in addition to the model approach, refer to the details in recognizing the spatial distribution of GWD and their spatial changes. In fact, the groundwater balance model is much simpler than a groundwater flux model, requires less data, and is easier to apply and to interpret results, but produces only lumped results of the groundwater budget and GWD, thus not reflecting the respective spatial distribution. When applying MODFLOW it represents a step ahead in recognizing the groundwater behaviour because knowing the variation of GWD in time and space is important to support decision making on water management. However, the successful assessment of changes in groundwater dynamics through the analysis of groundwater balance is in the origin of the present assessment, helped the formulation of hypothesis and allowed a simpler formulation of scenarios. Under these circumstances, both modelling approaches are compared relative to the results of assessing impacts of water saving measures on the groundwater behaviour.

Taking into account the considerations above, this paper aims at assessing the impacts of various irrigation water-saving practices and groundwater abstraction on the groundwater dynamics in the Jiefangzha Irrigation System (JFIS) of Hetao, Yellow River basin. An integrated methodology based on loose coupling of a purposefully modified version of MODFLOW and GIS is applied, which includes changes in the evaporation algorithm. In addition, this study is also aimed at supporting the identification of measures and future research issues that should provide for an appropriate adoption of foreseen water-saving measures and practices, which could lead to improving land and water use in this arid region.

2 Study Area

2.1 Location, Climate, Soils and Irrigation

The Hetao, located in the arid upper reaches of the Yellow River, is one of the three largest irrigation districts of China. It covers an area of 1.12 Mha. 570,000 ha are irrigated and the remaining area is occupied by towns and villages, roads and hydraulic infrastructures, sand dunes and salty badlands and wetlands. The Hetao is one of the most important food production bases in Northwest China, producing 35% of wheat, 37% of sunflower and 36% of sugar beet of the Inner Mongolia autonomous region (Wang et al. 1993; IWC-IM 1999). About 5.2 billion m^3 of water are diverted each year from the Yellow River to irrigate this area (IWC-IM 1999; Hetao Administration 2003). According to the management plans of the Yellow River Water Conservancy Commission, those irrigation water diversions shall reduce to less than 4.0 billion m^3. Therefore, water-saving practices are definitely required.

The JFIS is one of the Hetao irrigation systems and is taken as case study. The main part of the JFIS is located southeast of the main drainage ditch and northwest of the main canal (Fig. 1). It is bounded by the fourth sub-main drainage ditch and the Yongji sub-main canal in the east, and by the first sub-main drainage ditch and the Wulahe sub-main canal on the southwest border. The JFIS is the second largest system in the Hetao, with a total area of 215,700 ha, of which 66% is irrigated. It has a flat topography, with an average slope of 0.02% from southeast (SE) to northwest (NW).

The study area has a typically arid continental climate. The mean annual precipitation for the period of 1986–2004 is only 155 mm, with 70% of rainfall occurring from July to September. The monthly temperature averages are −10.1 and 23.8°C in January and July, respectively. The mean annual evaporation is about 2000 mm, thus much larger than precipitation. There are 135–150 frost-free days and 3100–3300 sunshine hours per annum.

The soil usually begins to freeze by the middle of November and does not thaw completely until late April (Wang and Akae 2004). The largest frozen depth is about 1.10 m by mid March. Soils in the southern part are alluvial silt sediments with sandy loam to silt loam texture, while in the northern part they are formed by lake and alluvial sediments with more fine textures such as silty and clay soils (Xu et al. 2010).

Wheat and maize are the main food crops, and sunflower, oil seeds and sugar beet are the main cash crops in JFIS. Due to the climatic conditions in the region, irrigation is essential during the entire crop growing season. Irrigation water is mainly

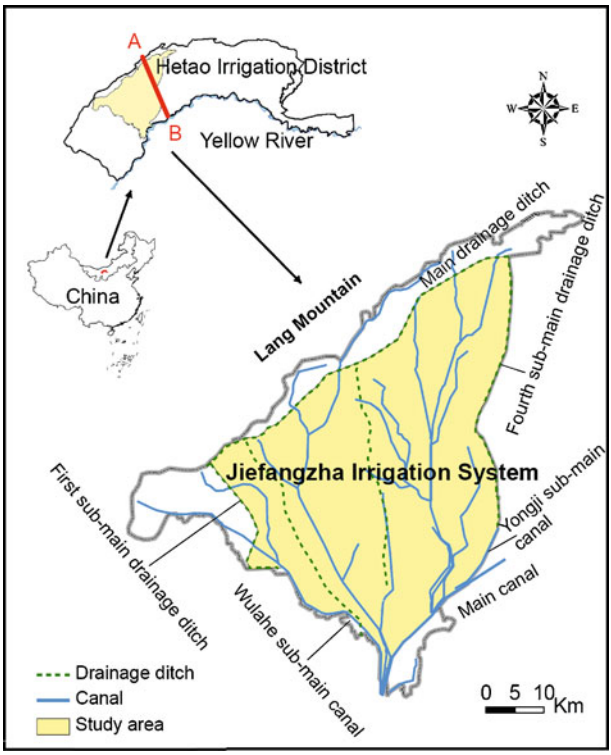

Fig. 1 Location of the study area and identification of the transept **a**–**b** described in Fig. 2

diverted from the Yellow River. Due to the very high charge of sediments, surface basin irrigation is the major irrigation method. Groundwater is mainly exploited for domestic and industrial purposes. Canal seepage and field percolation cause the rising of the groundwater table and associated soil salinity. Similar conditions were observed in the nearby Huinong irrigation district (Hollanders et al. 2005; Pereira et al. 2007; Gonçalves et al. 2007) and in the Yanqi basin in Northwest China (Brunner et al. 2007). Groundwater is either used by the crops through capillary rise or, due to the poor drainage system, is discharged by evaporation that causes severe problems of soil secondary saline-alkalization (Wang et al. 1993; Hillel 2000). Recent remote sensing studies give evidence of the great dimension of salinity problems in Hetao (Wu et al. 2008; Yu et al. 2010). In JFIS, the wasteland salt affected area was about 16% of the total area. In addition, 11% of the crop area has severe salt problems that highly impact yields, and near 25% of the cropped area was affected by salinity but to a lesser degree (IWC-IM 1999). The study by Yu et al. (2010) shows that the salinity affected area in JFIS is decreasing after improved drainage and consequent lowering of the GWD. Soil salinity is lower where GWD is deeper (Yu et al. 2010). This improvement is possible when water-saving irrigation practices and improved drainage are adopted, thus reducing percolation and seepage to the groundwater. Percolation associated with the autumn irrigation is particularly important (Feng et al. 2005), which is considered in this study independently of crop season irrigation. However, an excessive lowering of the water table will negatively impact vegetation growth due to reducing capillary rise. The most appropriate target

Table 1 Target groundwater table depth in the Jiefangzha Irrigation System (Ruan et al. 2008)

Period	Dates	Target depth (m)
Thaw to first irrigation	April	2.4–2.0
Crop growth period	May to mid September	2.0–1.5
Harvest to autumn irrigation	Late September to late October	2.0–2.4
Autumn irrigation to frozen	Early November to Mid November	1.3–1.7
Frozen to thaw	Late November to end March	1.7–2.4

GWD that satisfy conditions referred above are shown in Table 1 relative to different seasons. These data results from former studies (Ruan et al. 2008); GWDs proposed by these authors are larger but not in disagreement with those proposed for the nearby Huinong irrigation system (Hollanders et al. 2005; Pereira et al. 2007). However, drainage conditions need to be upgraded to achieve those target depths.

2.2 Hydrogeology

The Hetao was formed at the late Jurassic and is a closed rift basin. This basin is underlain by Quaternary sediments, mainly lake sediments and alluvial deposits of the Yellow River. The Quaternary systems in JFIS become thicker from south to north where regional subsidence has occurred. As schematically represented in Fig. 2, the thickness of Q4 (Holocene) ranges 6–25 m, while that of Q3 (Upper Pleistocene) varies from 35 to 240 m in the southeast–northwest (SE–NW) direction. Two aquifer groups are identified (Fig. 2). The first one is composed of two water-bearing strata (Q4 and Q3), and consists of an unconfined aquifer, that is under major exploitation. The deposits properties for Q4 are mainly sandy loam in the south and clay with interlayers of silt sand in the north, while the deposits properties

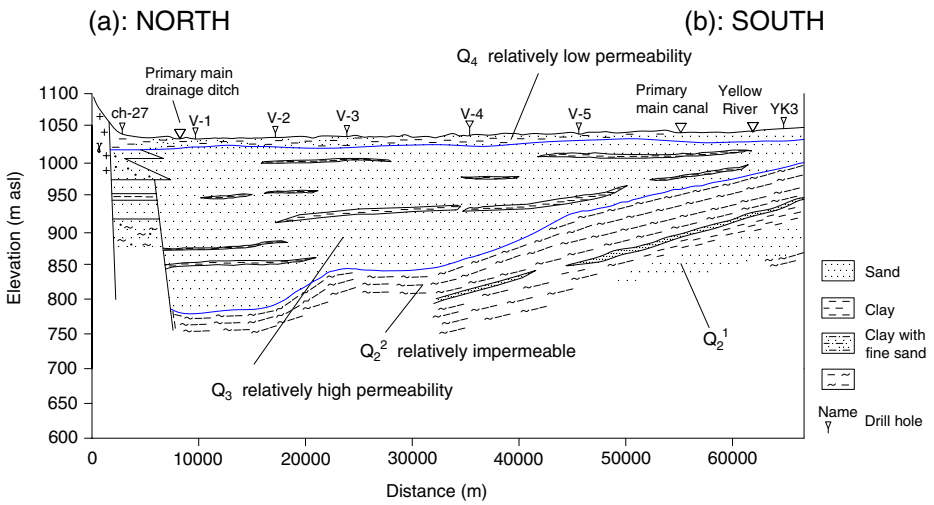

Fig. 2 South–north schematic hydrogeological cross-section of the aquifer system in the Hetao Irrigation District (the location of the **A**–**B** cross-section is shown in Fig. 1). ch-27, V-1 to V-5 and YK3 identify drill holes

for Q3 consist of fine-medium sand, fine sand and silt sand with clay interlayers. The Q4 stratum has a lower permeability with vertical hydraulic conductivity of about 0.03–0.1 m d^{-1} in the north–south (N–S) direction. The Q3 stratum has a relatively higher permeability, with a horizontal hydraulic conductivity of 4–18 m d^{-1} in the N–S direction. Therefore, Q4 and Q3 can be considered respectively as the first and second sub-aquifers of the first aquifer group.

The second aquifer group consists of the third water-bearing strata (Q2, Middle Pleistocene) (Fig. 2). The upper layer of Q2 (Q_2^2) is a layer of stable muddy clay with a thickness of 20–40 m, which acts as a low permeable layer preventing vertical flow. The lower layer of Q2 (Q_2^1) is mainly composed of sand and is highly permeable. It is confined and is not yet under exploitation. There is no hydraulic connection between the first and second aquifer groups due to presence of the Q_2^2 stable clay layer forming an aquitard. The first aquifer group interacts closely with surface water (Bameng Survey 1994). Salt accumulation occurred in Q3 during the Pleistocene (Wang et al. 1993). Continuous irrigation with excessive water amounts, thus producing large percolation to the groundwater, associated with high evaporation rates has caused a significant salt accumulation in farmland where groundwater is near the surface.

The direction of groundwater flow in the first aquifer group is shown in Fig. 3. This map was obtained from analyzing the dynamics of GWD observed in 56 observation wells and related hydrogeological information. The JFIS staff has monitored the groundwater table manually once every 5 days since 1950s. Data shows that the ground water flows from the main canal, in the southeast, towards the main drainage ditch, in the northwest. The hydraulic gradient of the groundwater is about 1/3000–1/5000, which is approximately the same as the slope of the ground surface. A

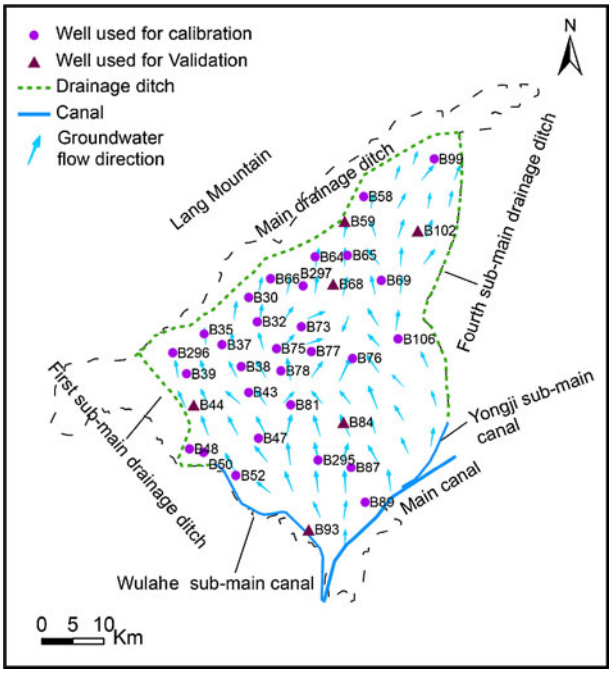

Fig. 3 Locations of observation wells used for model calibration and validation, and spatial information on groundwater flow directions relative to the first aquifer group

groundwater depression cone appears in the central part of this area due to intensive groundwater abstraction for industrial, domestic and livestock use by the Shanba town, Hangjinhouqi county.

3 Modelling Approach

3.1 Model Adaptation to Groundwater Dynamics Conditions Observed in Hetao

The modular finite-difference groundwater flow model MODFLOW-2000 (Harbaugh et al. 2000) was selected to simulate the behaviour of groundwater flow in the study area because it is a well-documented and extensively tested model, which can be readily incorporated into future studies for optimal water resources management. The MODFLOW model consists of a main program and various packages (McDonald and Harbaugh 1988). Those used in this study include Recharge (RCH), Well (WEL), River (RIV), Drainage (DRN) and Evapotranspiration Segments (ETS1). The Visual MODFLOW (Waterloo Hydrogeologic Inc. 2006) version 4.2 was adopted to simulate three-dimension unsteady groundwater flow in this study. Further model description and its coupling with GIS are presented by Xu et al. (2009). Step forwards in modelling relative to the former study are described below.

Groundwater evaporation (directly and through plant roots uptake due to capillary rise) is treated as a head-dependant flux boundary in MODFLOW. In the EVT package, which has been commonly used before, the functional relationship between GWD and evapotranspiration rate (ET) is simply expressed as a linear function. However, this relationship is not linear but can be expressed as an exponential curve for most conditions (Gardner 1958; Warrick 1988; Shah et al. 2007), including in arid and semiarid areas. Instead, the ETS1 package (Banta 2000), which uses a sequence of linear functions to describe that relationship, was therefore adopted. The datasets collected in JFIS (Wang et al. 1993; IWC-IM 1999) show that the functional relationships between the GWD and the ET ratio QET/QETM, between the actual and maximum groundwater evapotranspiration rates, are non-linear and can be described as piecewise linear functions (Fig. 4). These results are in agreement with those obtained by Brunner et al. (2008). In this study, QET was estimated for seven GWDs—0.5, 1.0, 1.5, 1.8, 2.1, 2.5, and 3.0 m—using datasets collected from experiments conducted in vegetated and non-vegetated lysimeters with two typical soils, a loamy and a silt–clay soil, at the Shahaoqu Experiment Station, located in the JFIS (Wang et al. 1993; IWC-IM 1999). QETM were estimated as the product of an empirical experimental coefficient by the evaporation rate from an open water surface (IWC-IM 1999). The piecewise linear functions match well the monthly observation data of this evaporation experiment for late April to October, e.g., data for September in Fig. 4.

The fact that the water table is above the ground surface in low lands is not well treated in MODFLOW and causes a poor build-up of head in those areas, mainly in the NW part of JFIS, particularly during the irrigation periods when percolation and seepage to the groundwater are larger. To prevent this to happen, in each time step, if water table is below or changes to below the land surface, the original value of specific yield is used. Whereas, if the water table was above the ground surface,

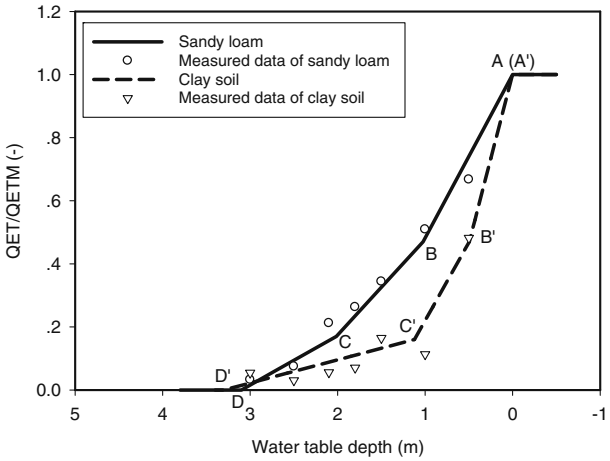

Fig. 4 Piecewise linear functions relating the evapotranspiration ratio QET/QETM between the actual and maximum groundwater evapotranspiration rates with the water table depth for sandy loam and clay soils (data refer to September)

the specific yield will be switched to values close to 1 in the corresponding cells. Accordingly, the storage term in both the finite difference equations and water budget calculations was modified for these cells. These modifications were performed assuming that the process occurs in land depressions, where water remains on the land and does not runs off. This assumption is appropriate because land is flat.

3.2 Data and Model Setup

Data used in MODFLOW consist of: the aquifer-system stress factors, the aquifer-system and strata geometry, the hydrogeological parameters of the simulated process, and the main measured variables. Stress factors include the pumping volume, effective recharge, groundwater evaporation (i.e., direct evaporation and vegetation root uptake due to capillary rise), and groundwater–surface flow exchanges. They were imposed to the model through the boundary conditions or sink/source terms using the boundary packages of MODFLOW. The aquifer-system geometry was determined using the available geological information (e.g. boreholes data and cross sections) and topographic maps. The hydrological parameters, including hydraulic conductivity, specific storage and specific yield, were obtained using raw data and the interpolation method. The main measured variables were the groundwater heads at specified points and different time periods, and related data were used for model calibration and validation. Details on the aquifer discretization, initial and boundary conditions and further modelling are presented by Xu et al. (2009).

The recharge from canal seepage, C_r, rainfall, P_r, and deep percolation from field irrigation I_r during the crop growth and irrigation period were estimated (IWC-IM 1999; Hetao Administration 2003) respectively as:

$$C_r = bQ_{cd} \tag{1}$$

$$P_r = dPA \tag{2}$$

$$I_r = caQ_{cd} \tag{3}$$

where Q_{cd} is the inflow rate of a canal, b is the canal seepage ratio, d is the rainfall recharge coefficient, P is the cumulative precipitation considering only the rainfall events ≥5 mm, A is the rainfall recharge area, i.e., excluding the area occupied by residential land, roads, canals and drainage ditches; a is the canal conveyance ratio relating outflow to inflow discharges; and c is the deep percolation ratio referring to the total irrigation water applied to a field. The time step computation is the day and therefore units for the variables are $m^3\ day^{-1}$. The initial values of the empirical coefficients a, b, c, d for different reaches of each canal and recharge zones were available from previous studies (IWC-IM 1999; Hetao Administration 2003; Wei 2003; Yang 2005).

The recharge due to canal seepage from high-order canals assigned to the cells through which the canal water is flowing was computed with the RCH Package. Recharge from field percolation, rainfall, melt water (estimated as the product of the specific yield S_y by the changes in GWD during that melting period), and canal seepage were combined into a single effective recharge R_e, also using the RCH Package. It was assumed that groundwater recharge in residential areas is negligible.

The evaporation from the groundwater depends mainly from the evaporative demand of the atmosphere and GWD, which control capillary rise. With the ETS1 package, the piecewise linear ET functions were defined by using the proportion of extinction depth (PXDP), i.e., the GWD when ET becomes null (Shah et al. 2007), and the proportion of maximum ET rate (PETM) (Banta 2000). Piecewise linear functions with three segments were used to characterize the groundwater ET from May to early November for sandy loam and clay soils (Fig. 4). The values of PXDP and PETM for the points A, B, C, D, A′, B′, C′, and D′ in Fig. 4 are presented in Table 2. Groundwater ET in residential areas and from ditches and canals was neglected because it is much smaller than that from agricultural and natural areas. During the soil frozen period, ET from the groundwater was estimated as a function of temperature, GWD, and S_y following the empirical procedure proposed by Wang et al. (1993).

The groundwater abstraction for industrial, domestic and livestock uses was estimated with the WEL Package with appropriate spatial distribution. The estimation based upon the industrial output per unit of water used, the population at each locality and related daily demand per capita, and the livestock dimension and respective demand per livestock head.

The water discharged into the drainage ditches primarily consists of excess irrigation water, industrial and domestic drainage and groundwater natural discharge. Only the main and sub-main drainage ditches (Fig. 1) were considered for estimating the groundwater natural discharge; the DRN Package was used for this purpose.

Table 2 The proportions of extinction depth (PXDP) and maximum evapotranspiration rate (PETM) for sandy loam and clay soils in the JFIS (Points A, B, C, D, and A′, B′, C′, D′ are identified in Fig. 4)

	Sandy loam				Clay soil			
	A	B	C	D	A′	B′	C′	D′
PXDP	0	0.33	0.65	1	0	0.15	0.34	1
PETM	1	0.47	0.17	0	1	0.47	0.16	0

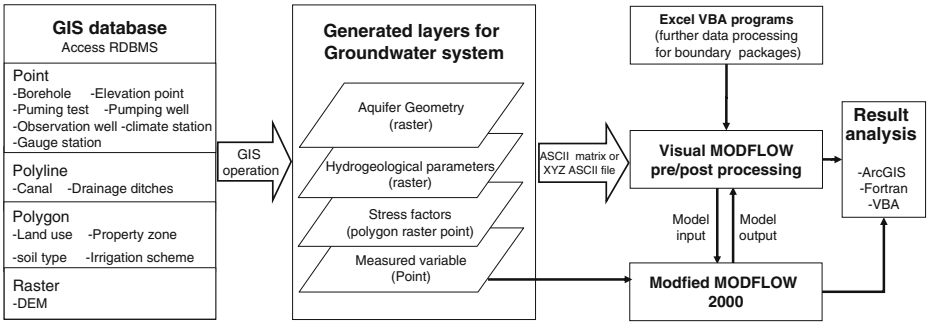

Fig. 5 Schematic representation of the procedures used for GIS data processing and construction of the databases for the groundwater flow model

3.3 Data Processing Using GIS

The ArcInfo version 9.2 (Environmental Systems Research Institute, ESRI) with Access databases (Microsoft) was used to construct the GIS database (Xu et al. 2009). Main features are summarized in Fig. 5.

A digital elevation model (DEM) in 90 m of spatial resolution was obtained from the International Centre for Tropical Agriculture (Jarvis et al. 2006). The DEM was resampled to 200 × 200 m, which was the grid adopted for MODFLOW. Considering the influences of DEM accuracy on the estimation of groundwater ET (Li et al. 2008), 103 sets of benchmark surface elevation data available for the JFIS area were utilized to first compare with the DEM data (coefficient of regression of 1.00 and coefficient of determination of 0.97), which has shown appropriate accuracy, and then to combine with DEM data. Interpolation was performed using kriging. It produced a new and more accurate surface raster data with 200 meter resolution that was used with MODFLOW.

Data on 30 boreholes with attribute data of aquifer elevations and lithology, 25 pumping test sites with hydrogeological attribute data, 246 pumping wells with groundwater abstraction attribute data, and 35 observation wells used for calibration and validation (Fig. 3) and monitored once each 5 days, were imported as point format. Hydrographic information (distribution of canals, drainage ditches, water courses, and roads, and water administration maps), land use and salinity maps were incorporated as vectors in the GIS database. Using the 1:100,000 land use map of Hetao, land use was characterized in 9 categories: farmland, grassland, woodland, salt affected badland, dunes, open water, residential and construction areas, canals, and drainage ditches. Hydrogeological maps of Hetao at 1:100,000 scale were also included in the GIS database and used to obtain the hydrogeological property zones and parameters. Several hydrogeological cross-sections were available from previous studies (Wang et al. 1993; Bameng Survey 1994; IWC-IM 1999).

Meteorological data on monthly evaporation and rainfall were collected from the Hangjinghouqi and Linhe Weather Stations and six agrometeorological stations equipped with a rain gauge and a 20 cm evaporation pan. Spatialization was performed using the Thiessen polygons method applied to these 8 points. All spatial

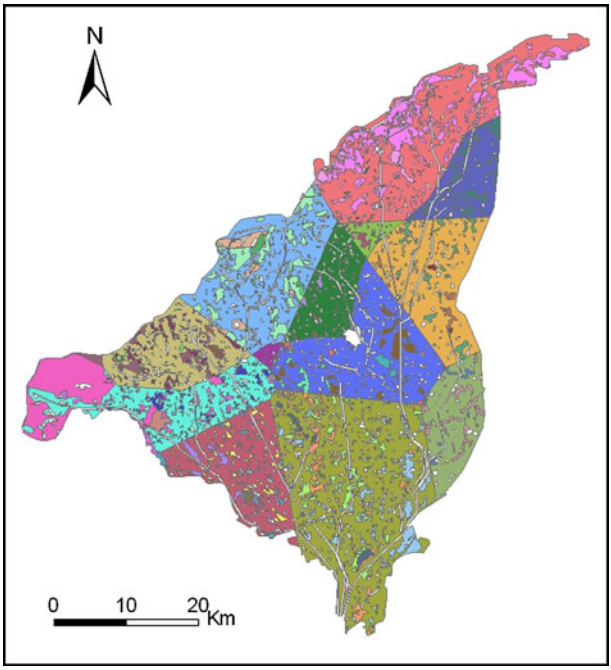

Fig. 6 Spatial distribution of the assigned 52 evaporation zones for using with the evapotranspiration package, where different *colours* represent different zones

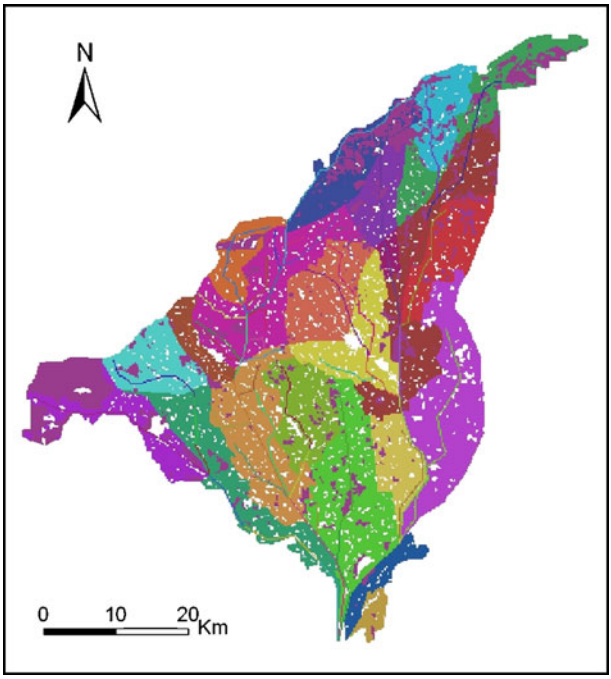

Fig. 7 Spatial distribution of the assigned 73 recharge zones for using with the recharge package, where different *colours* represent different zones

data of JFIS were integrated and stored in the geodatabase (MacDonald 2001). The topology, subtype and domain were created for accurately processing the spatial data for MODFLOW use. The geodatabase was connected with a database management system (Microsoft Access) for efficient management of the GIS database (Xu et al. 2009).

Combining the land use, soil type and climatic Thiessen polygons, 52 evapotranspiration zones were produced in polygon format based on extract and overlay functions (Fig. 6). Similarly, considering irrigation water, rainfall, and soil types, 73 recharge zones were defined in the RCH Package (Fig. 7).

The model results were displayed in Visual MODFLOW as contouring and colour filling maps. Various Fortran programs were developed to efficiently abstract and analyze output data of MODFLOW, which also are a step forwards relative to the study by Xu et al. (2009). These programs can automatically generate groundwater heads, dropdowns and GWDs in ASCII array format that can be directly used by ArcGIS. The spatial distribution of the GWDs can then be easily analyzed with appropriate ArcGIS tools.

4 Results and Discussion

4.1 Model Calibration and Validation

The parameters referring to the hydraulic conductivity, specific yield and recharge coefficient relative to irrigation water, because they were relatively uncertain in the study area, were calibrated through an iterative process. Groundwater level (GWL) and GWD data from 29 observation wells (Fig. 3) were used for model calibration. Computations relative to the groundwater head were performed using a daily time step; however, data were later aggregated into larger periods according to the nature of other variables used. The calibration was performed for the period from May 1, 2004 to April 30, 2005, and this period was divided into twelve stress periods, i.e., periods when model parameters can be assumed as constant (McDonald and Harbaugh 1988). During the irrigation season, from May 1 to October 31, each stress period was month duration, while out of this season the stress periods ranged from 10 to 60 days according to specific boundary conditions considering the climatic conditions and water recharge.

A trial and error method was used in the calibration process as advised by Hill et al. (2000). The root mean square error (RMSE), the standard error of the estimate (SEE) and the Nash and Sutcliffe model efficiency (EF) were used as indicators of goodness of fit (Legates and McCabe 1999; Moriasi et al. 2007). In addition, a regression forced to the origin comparing the observed and simulated monthly GWL and GWD was also used (Fig. 8). Both regressions show good agreements between measured and simulated GWLs (Fig. 8a) and GWDs (Fig. 8b), with $b = 1.0$ and $R^2 = 0.98$ relative to GWL and $b = 0.98$ and $R^2 = 0.86$ relative to GWD. RMSE, SEE and EF for GWL are 0.34 m, 0.019 m and 0.98, respectively.

Xu et al. (2009) obtained RMSE = 0.44 m, SEE = 0.025 m and EF = 0.97 from twelve observation wells when calibrating the former version of the model, which are inferior to those referred above. Results obtained with the previous and the presently modified model version were also compared for two wells selected randomly (B43

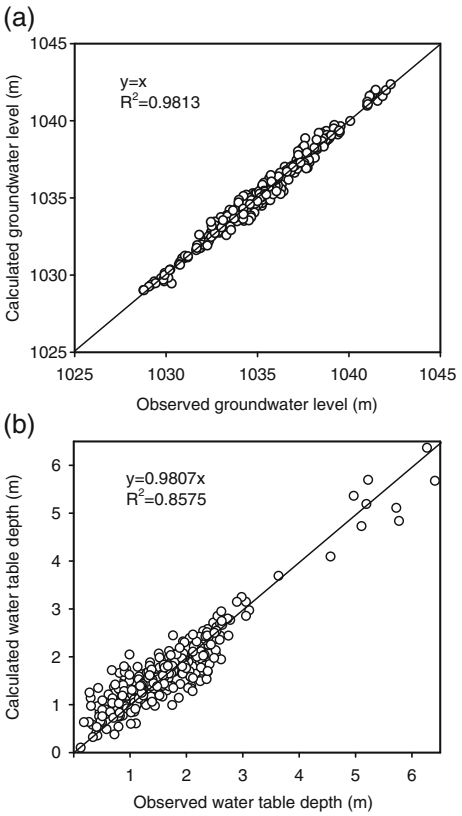

Fig. 8 Relationship between the observed and calculated monthly means of the groundwater levels (**a**) and groundwater depths (**b**) for the 29 observation wells used for calibration

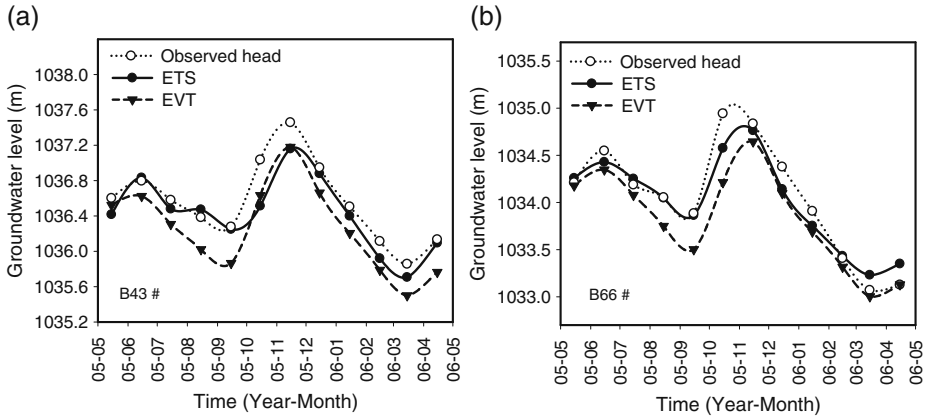

Fig. 9 Observed and simulated groundwater levels at two selected observation wells B43, in a sandy loam soil (**a**), and B66 silty–clay soil (**b**) comparing results of using the EVT and ETS1 packages for ET simulation

and B66) in sandy–loam and silt–clay soils, respectively (Fig. 9). Results show that GWLs are simulated better when using the new ETS1 package relative to the former EVT, and that this superiority is not seasonal but is observed through the entire year, which indicates that the modified version of the model is effectively improved relative to the former.

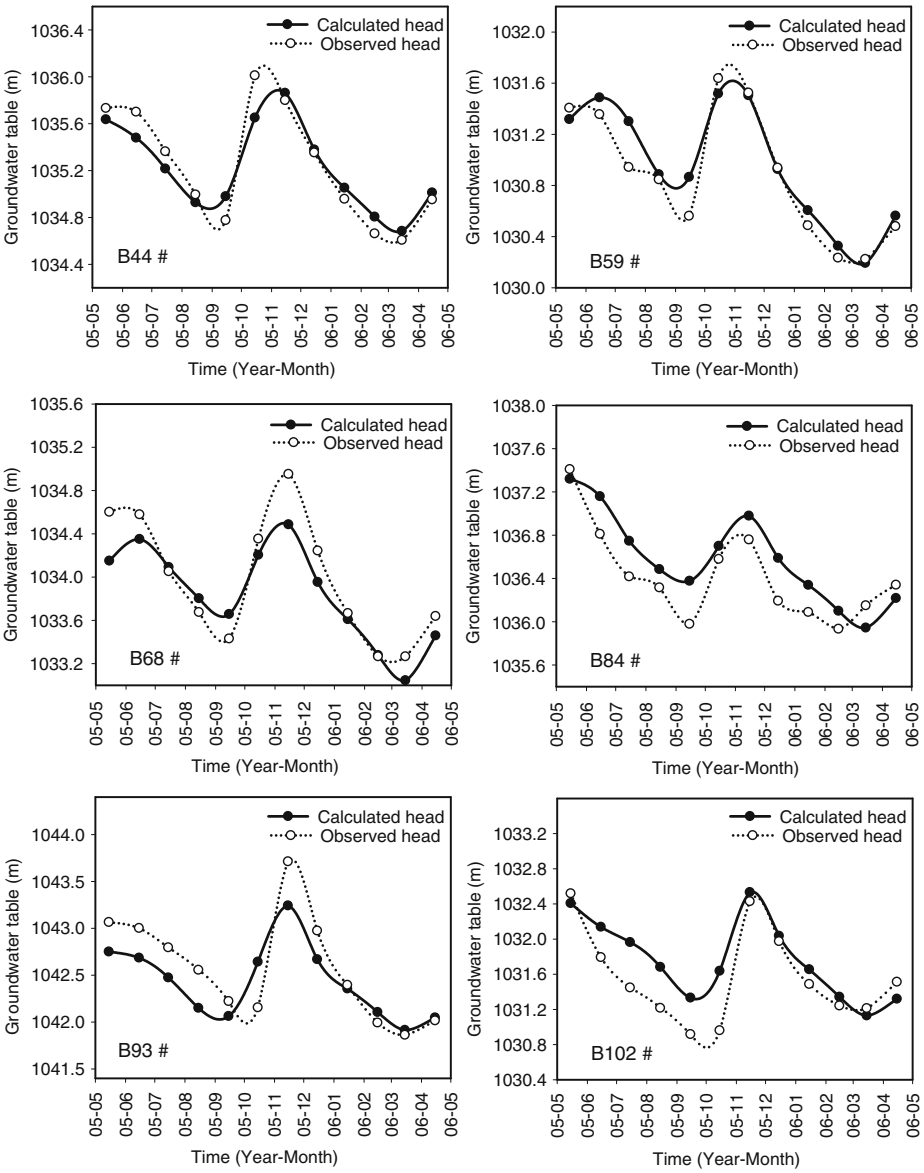

Fig. 10 Comparison of observed and calculated groundwater levels at the 6 observation wells used for validation

The model was validated with data of six different observation wells, whose locations are given in Fig. 3, for the period from May 1, 2005 to April 30, 2006. The same twelve stress periods defined for calibration were used for validation. All hydraulic parameters and empirical coefficients were the same as used for calibration. The simulated monthly GWL agree well with the measured data (Fig. 10), showing small errors of the estimate (RMSE = 0.23 m, SEE = 0.029) and high modelling efficiency (EF = 0.995), hence indicating that parameters were properly calibrated.

4.2 Predicting Impacts of Water Saving and Groundwater Use

4.2.1 Scenarios

Irrigation water-saving practices are being progressively implemented in Hetao. They include: (a) the improvement of the canal system, upgrading of canal control and regulation structures, and better canal water delivery structures and management; (b) upgraded irrigation scheduling, land levelling of irrigated fields, and improved furrowed and flat basin irrigation systems. The area under cultivation is supposed to be maintained, 146,100 ha in the study area. Groundwater abstraction will increase with the foreseen population growth, livestock augmentation and the development of industry. Groundwater is not foreseen to be used for irrigation. The groundwater abstraction by the year 2020 was estimated and considered for the prediction of changes in groundwater dynamics.

The canal system improvement is expected to reduce water conveyance losses, thus increasing the conveyance ratio (a) of the canal system and decreasing the seepage ratio (b) (Eqs. 1 and 3). According to findings reported by IWC-IM (1999), the parameter a is supposed to increase by 0.018 when the percentage of lining of the main and sub-main canals increases by 10%, and by 0.009 when the percentage of lining of tertiary and quaternary canals augments by 10%. Five scenarios for canal system improvement were considered, with 20, 40, 60, 80 and 95% of lining of the main, sub-main, tertiary and quaternary canals together with upgrading the respective hydraulic structures (Table 3). These resulted in increasing the a values from 0.49 at present to respectively 0.54, 0.57, 0.63, 0.69 and 0.75 in future. The value of 0.75 is reasonable when considering the studies by Xie et al. (2003), Li et al. (2004) and Gonçalves et al. (2007) for the nearby Huinong irrigation system. Resulting from canal system improvements, the seepage ratio (b) is expected to be reduced (IWC-IM 1999). According to Ruan et al. (2008), the ratio of canal seepage to the total canal conveyance losses ($b/(1-a)$) may be assumed as constant, thus b decreases proportionally to the increase in parameter a.

Table 3 Present situation and five scenarios for water saving in the JFIS

Scenarios	% of area with canal system improvements	% of area with upgraded irrigation technology
0	Present	Present
1	20	20
2	40	35
3	60	50
4	80	65
5	95	80

The percolation ratio (c) is assumed to decrease from 0.27 to 0.12 during the crop season and from 0.42 to 0.25 for the autumn irrigation period, corresponding to upgraded irrigation technology in 20 up to 80% of the irrigated area (Table 3). These values are coherent relative to the results presented by Pereira et al. (2007) and Gonçalves et al. (2007) for the Huinong irrigation system when farm systems are upgraded to a high level. Groundwater abstraction is assumed to increase 1633 to 4436 10^4 m^3a^{-1} from present to the year 2020, which is the time horizon for the changes. Therefore, five scenarios are considered corresponding to progressive improvements of the farm and off-farm systems (Table 3). Scenario 1 represents a consistent first step in irrigation system upgrading while scenario 5 corresponds to the maximum attainable level of improvement and to a quite large time span for implementation.

4.2.2 Groundwater Table Depth

The changes of GWDs predicted for the five scenarios indicate that the groundwater table will decline progressively with the application of water-saving practices and the increase of groundwater abstractions. Simulations for all scenarios were performed with 2004 data. The areas of JFIS where GWDs are in a given depth class are shown in Fig. 11 for June, July and August. Classes for groundwater depths are: very shallow (GWD $<$ 1.5 m), shallow (1.5 $<$ GWD $<$ 2.0 m), deep (2.0 $<$ GWD $<$ 3.0 m), and very deep (GWD $>$ 3.0 m).

The area with very shallow groundwater shows to steadily decrease from present 104,000 ha in June (Fig. 11a) down to 70,180 ha with scenario 5, i.e., from 57.9 to 39.1%. Contrarily, the areas with deep and very deep groundwater increase respectively from 33,044 ha to 51,000 ha and from 9,408 ha to 22,804 ha, that correspond to change from 18.4 to 28.4% and 5.2 to 12.7% in June (Fig. 11a, b). This increase in areas with deeper GWD could favour salinity control but could also lead to negative impacts due to reduced capillary rise for natural vegetation and crops, which may lead to requiring more irrigation water to effectively satisfy crop water requirements. Differently, the areas with shallow groundwater, where the target depth (1.5 $<$ GWD $<$ 2.0 m, Table 1) would be achieved during the crop growth season, tend to do not change appreciably in June and July (Fig. 11b, d). In August, this area where the target GWD is achieved tends to slightly decrease from scenario 1 to 5, the later showing a difference of about 4.5% relative to present, i.e., from 25 to 20.5% of the total area.

To be noted when comparing the monthly values that the areas with GWD $<$ 1.5 m are lesser in August than in June: 50.4% in June vs. 41.9% in August for present, and 30.2 and 23.2% for the same months considering scenario 5 (Fig. 11a, e). This variation is due to groundwater discharge by evaporation and plants uptake during the months with higher climatic demand for ET. A lowering of GWD from June to August was observed by Xu et al. (2010).

Analyzing results for scenario 5, it is apparent that the area with deeper GWD, i.e., larger than 2.0 m, would become the largest of JFIS, increasing by more than 1/3 relative to present. This indicates that the groundwater table is expected to significantly decline when water saving irrigation is adopted. However, this decline would be associated to a decrease of groundwater ET as analyzed in the next section.

Figure 12 shows the spatial distribution of the GWD in July for various scenarios. Presently, most area with GWD $<$ 1.0 m is in the northern and NW part of JFIS,

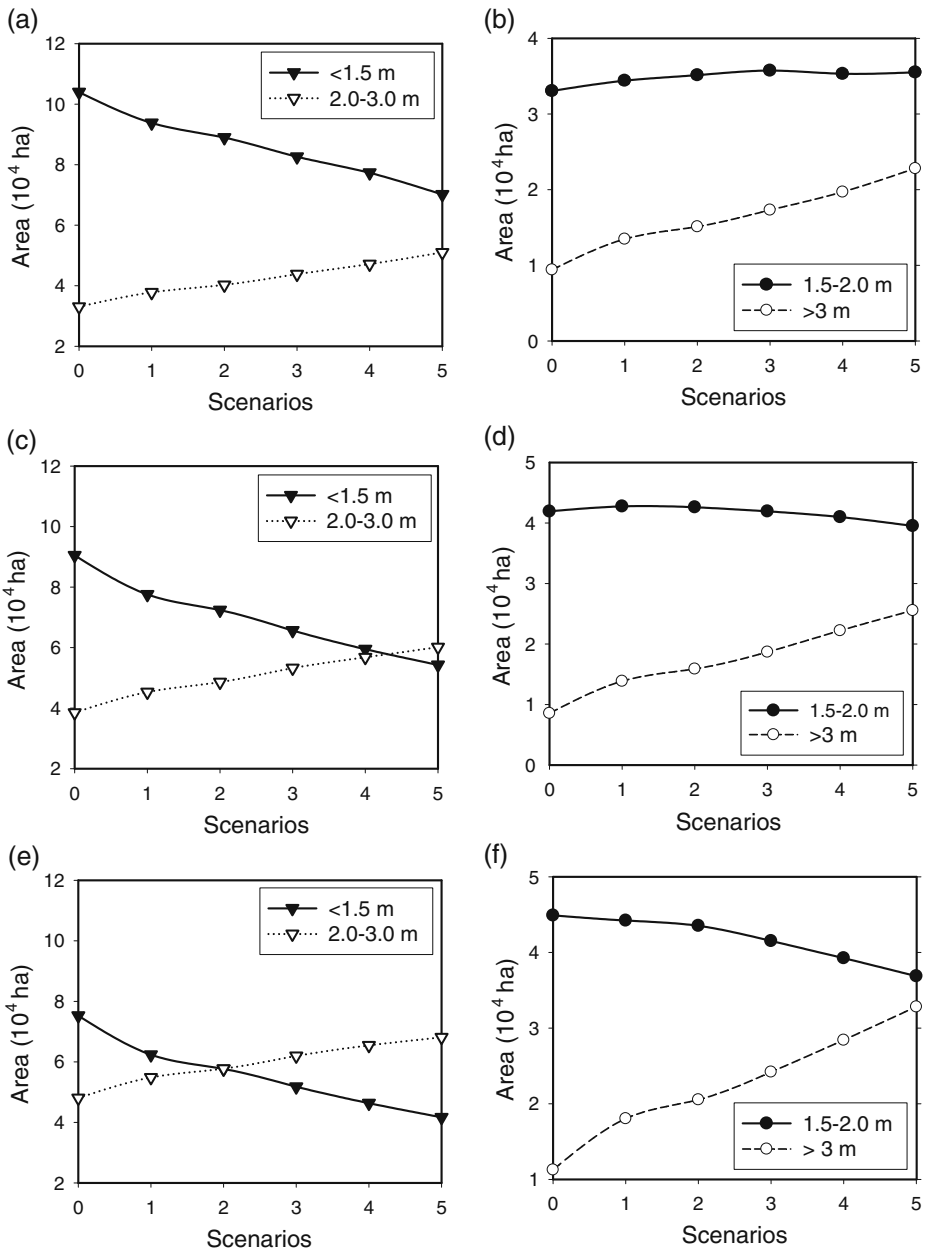

Fig. 11 Predicted areas having very shallow, shallow, deep and very deep groundwater table depths: comparison of the present situation (scenario 0) with those predicted for scenarios 1 to 5 in June (**a** and **b**), July (**c** and **d**), and August (**e** and **f**)

which relates with the fact that this area is of lower elevation and groundwater flows towards this area. This area is also that where most of saline and waterlogged fields are located. The areas having a deeper GWD are located in the southern and SE

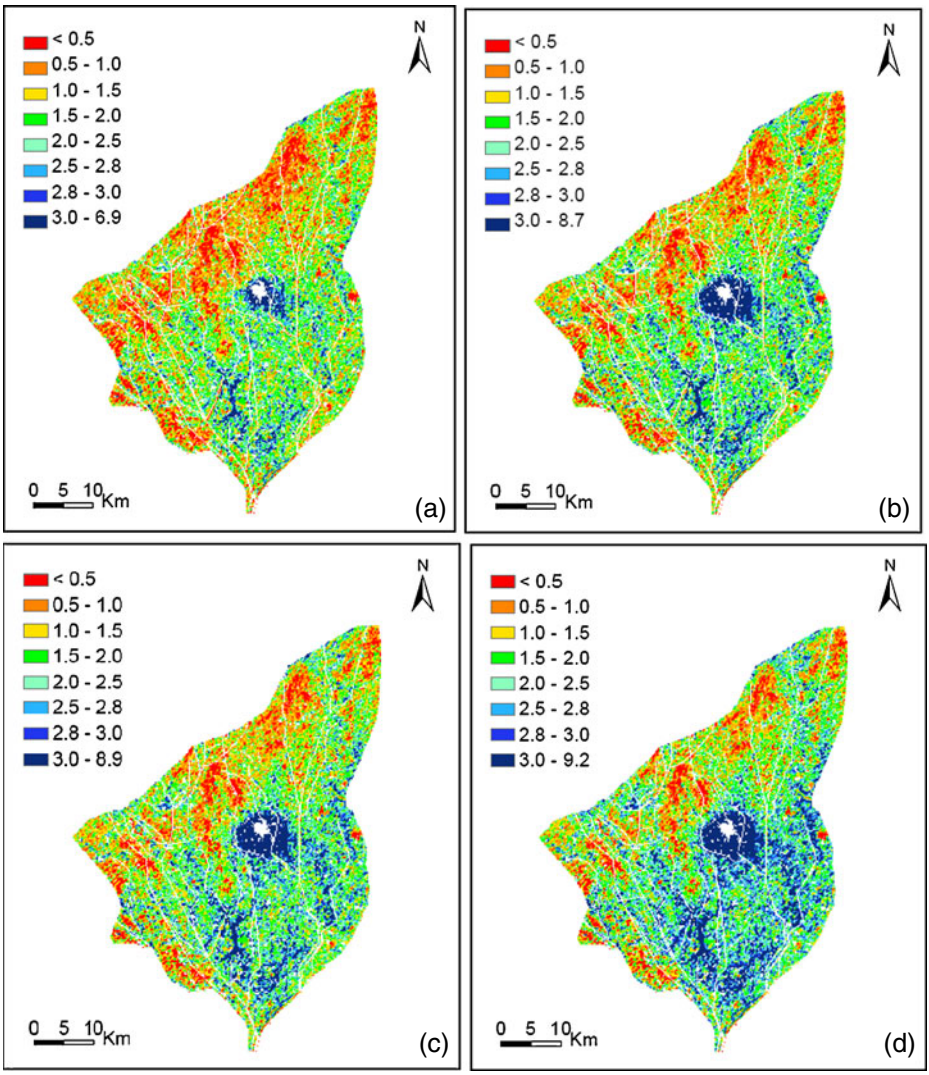

Fig. 12 Spatial distribution of the groundwater table depth in July for: the present situation (**a**), and for scenarios 2, 3 and 5, respectively (**b**), (**c**) and (**d**)

parts of JFIS. These areas are also closer to towns and other settlements where groundwater abstraction favours GWD deepening. Only small areas in the central and southern parts have a GWD close to or larger than 3.0 m. A groundwater depression cone occurs in the central part, around Shanba town, Hangjinhouqi county, caused by the large groundwater abstraction there. The application of water-saving practices can increase the area with suitable GWD in the NW (Fig. 12b, c, d) but the groundwater table decline is expected to be larger in S and SE, resulting in a large area with a depth close to or larger than 3 m. Results for the scenario 5 indicate a large decrease of the GWD and a larger area with a deeper GWD. These spatialized

results allow identifying the areas where negative impacts on vegetation growth are expected due to reduced capillary rise in S and SE regions. It becomes also possible to identify the areas where the water table decline will favour the rehabilitation of salt affected lands, especially in the northern region.

Results are not comparable with those of the groundwater balance in Xu et al. (2010) because these are lumped while MODFLOW results are distributed. However, results of both approaches are coherent.

4.2.3 Groundwater Balance

The terms of the groundwater balance during the irrigation period, May to early November, were calculated for the present situation and the five scenarios (Fig. 13). Results show that recharge from irrigation water and groundwater discharge through evaporation and plant roots uptake are the main terms of the water balance and those having a major influence on the variations of the groundwater levels as shown in Fig. 10. Canal seepage and field percolation are the most important sources of groundwater recharge, respectively 119 and 115 mm at present, which account respectively for 49.4 and 47.8% of the total recharge. The recharge from the precipitation is very small, 6.5 mm. The main groundwater discharge is groundwater ET (direct evaporation and uptake by vegetation), which presently accounts for 176 mm, i.e., 87% of the total discharge during the irrigation period. Groundwater abstraction and discharge by drainage account for only 5.5 and 7.3% of the total discharge, respectively.

A reduction of groundwater evaporation is predicted when water saving measures are implemented (Fig. 13). Compared with the present, scenarios 1 to 5 could reduce groundwater evaporation by 21 to 63 mm. This reduction in evaporation should help controlling secondary salinization; however, the contribution of capillary rise for vegetation water use also decreases. Simultaneously, the recharge from the irrigation water is expected to decrease by 28 to 133 mm for scenarios 1 to 5, thus by 12% to 57% relative to present. These results explain the foreseen lowering of GWDs. The proportion of groundwater abstraction to the total discharge is

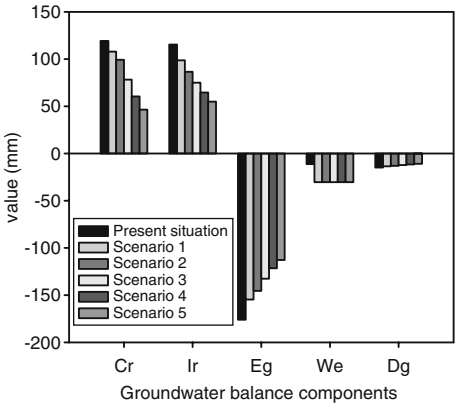

Fig. 13 Groundwater balance components during the irrigation period for the present and for the scenarios 1 to 5: C_r is the recharge from canal seepage (mm), I_r is the recharge from field percolation (mm), P_r is the recharge from rainfall (mm), E_g is the groundwater evaporation (mm), W_e is the groundwater abstraction (mm), D_g is the groundwater discharge through the drainage ditches (mm)

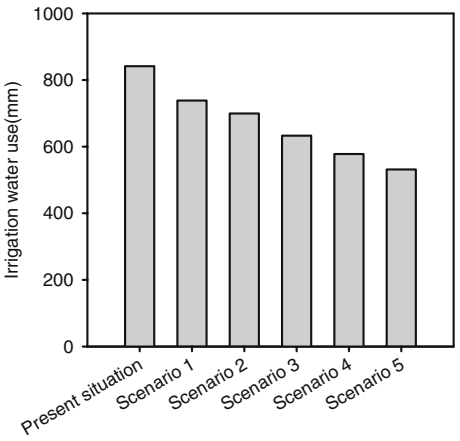

Fig. 14 Irrigation water use during the crop growth season and autumn irrigation period for the present situation and predicted for scenarios 1 to 5

expected to largely increase, from 5.5% to 19.7%, to satisfy the demand for industrial, domestic and livestock uses. This would also contribute to the lowering of GWDs as referred before.

Scenarios 1 to 5 correspond to various time and space steps for the implementation of water-saving measures. As shown in Fig. 14, the demand for irrigation water shall progressively decrease from 842 mm at present to 532 mm for scenario 5. However, it is likely that upgraded crop husbandry and new varieties of crops will be considered together with the water-saving measures. Then, crop consumptive water use may increase relatively to present while non-beneficial water uses, e.g. seepage, deep percolation and non-crop evaporation (Pereira et al. 2009) are expected to decrease, which may result in that those decreases may be less drastic than current forecasts.

The results obtained by Xu et al. (2010) using a lumped groundwater balance model are comparable with the forecasted canal seepage, field percolation and groundwater evaporation. The results of both models indicate that a high level of water-saving practices might result in too much deep GWD, with subsequent lower capillary rise contributing to crop growth. Results indicate the need of research to better characterize the parameters relative to conveyance, seepage and percolation ratios as well as irrigation demand in the area.

In this study, modelling results clearly indicate the magnitude of expected changes when water-saving measures are adopted at both the canal system and the farms. These changes call for further investigations relative to crop and irrigation management when the increase of GWDs will provide for smaller groundwater contribution for the vegetation. In addition, since the water table will be lower in areas where it is currently high and soils are saline, some priority must be given to investigate on the rehabilitation of these soils, including through crop husbandry and drainage. Moreover, because the results of modelling are spatialized, their analysis should provide for further defining the priority areas for implementation of water-saving measures, as well as for identification of difficulties associated with the groundwater dynamics resulting from the implementation of those measures.

5 Conclusions

Coupling the groundwater flow model MODFLOW with a GIS database allowed to simulate the groundwater dynamics in the Jiefangzha Irrigation System, Hetao Irrigation District, in the arid upper Yellow River basin. The calibration and validation of the model provided for an adequate parameterization relative to the processes influencing the groundwater recharge and discharge as influenced by irrigation. The model and corresponding methodology were then used to simulate the groundwater dynamics of the study area for various water-saving practices with considering the groundwater abstraction foreseen for the year of 2020. Results show that the water-saving practices with 60% of canal lining and upgrading hydraulic structures, and improved farm irrigation technology in 50% of the area constitute a reasonable solution. Their implementation would lead to reduce groundwater evaporation by 43 mm and the total diversions from the Yellow River by 208 mm.

Spatialized results show that the application of water-saving practices and the increase of groundwater abstractions will result in the decline of the groundwater table. In some areas this decline could be excessive since it leads to a large decrease of the groundwater contribution to the vegetation consumptive water use. In other areas with a shallow groundwater depth, the foreseen changes are expected to provide for improved cropping conditions and the control of salinity. Overall, relatively important decreases in diversions of water from the Yellow River are expected. However, it is necessary to recognize the limitations of these modelling studies since the parameterization of considered scenarios may differ from the future reality. In fact, different upgraded crop husbandry and new crop varieties are expected to be considered together with the implementation of water-saving measures. This calls for an appropriate follow-up when these measures are being implemented. Results also indicate the need for further investigations on crop water use aiming at reducing the non-beneficial uses of water and maximizing the beneficial ones, as well as on the rehabilitation of saline soils.

Acknowledgements This research was jointly supported by the National Science Foundation of China (grant numbers: 50979106, 50779067, 50669005, 51069006), the 12th Five-year Research Program of Ministry of Science and Technology, the Program for Changjiang Scholars and Innovative Research Team in University, and the Program of Beijing Key Subject of Hydrology and Water Resources. The support by the bilateral China–Portugal research cooperative Project is acknowledged.

References

Bameng Survey (1994) Researches on the water resources and salinization control system management model in Hetao Irrigation District of Inner Mongolia. Bameng Hydrology and Water Resources Survey Teams of Inner Mongolia, Hohhot (in Chinese)

Banta ER (2000) Modflow-2000, the US Geological survey modular ground-water model—documentation of packages for simulating evapotranspiration with a segmented function (ETS1) and drains with return flow (DRT1). US Geological Survey Open-file Report 00-466, Reston, Virginia

Brodie RS (1998) Integrating GIS and RDBMS technologies during construction of a regional groundwater model. Environ Modell Softw 14:119–128

Brunner P, Li HT, Kinzelbach W, Li WP (2007) Generating soil electrical conductivity maps at regional level by integrating measurements on the ground and remote sensing data. Int J Remote Sens 28:3341–3361

Brunner P, Li HT, Kinzelbach W, Li WP, Dong XG (2008) Extracting phreatic evaporation from remotely sensed maps of evapotranspiration. Water Resour Res 44:W08428. doi:10.1029/2007WR006063

Cai LG, Mao Z, Fang SX, Liu HS (2003) The Yellow River Basin and case study areas. In: Pereira LS, Cai LG, Musy A, Minhas PS (Eds) Water saving in the Yellow River Basin: issues and decision support tools in irrigation. China Agricultural Press, Beijing, pp 13–34

Dawoud M, Darwish M, El-Kady M (2005) GIS-based groundwater management model for Western Nile Delta. Water Resour Manage 19(5):585–604

Deng XP, Shan L, Zhang HP, Turner NC (2006) Improving agricultural water use efficiency in arid and semiarid areas of China. Agric Water Manage 80:23–40

Fang S, Chen X (2001) Rationally utilizing water resources to control soil salinity in irrigation districts. In: Stott DE, Mohtar RH, Steinhardt GC (Eds) Sustaining the global farm. Purdue University, pp 1134–1138

Feng ZZ, Wang XK, Feng ZW (2005) Soil N and salinity leaching after the autumn irrigation and its impact on groundwater in Hetao Irrigation District, China. Agric Water Manage 71:131–143

Gardner WR (1958) Some steady-state solutions of the unsaturated moisture flow equation with application to evaporation from a water table. Soil Sci 85:228–232

Gogu RC, Carabin G, Hallet V, Peters V, Dassargues A (2001) GIS-based hydrogeological databases and groundwater modelling. Hydrol J 9:555–569

Gonçalves JM, Pereira LS, Fang SX, Dong B (2007) Modelling and multicriteria analysis of water saving scenarios for an irrigation district in the upper Yellow River Basin. Agric Water Manage 94:93–108

Harbaugh AW, Banta ER, Hill MC, McDonald MG (2000) MODFLOW-2000, the US Geological Survey modular groundwater mode—user guide to modularization concepts and the groundwater flow process. US Geological Survey Open-File Report 00-92, Reston, Virginia

Herzog LB, Larson DR, Abert CC, Wilson DS, Roadcap SG (2003) Hydrostratigraphic modelling of a complex, glacial-drift aquifer system for importation into MODFLOW. Ground Water 41(1):57–65

Hetao Administration (2003) The datasets of evaluation of irrigation water use efficiency in Hetao Irrigation District of Inner Mongolia. Hetao Irrigation Administration Bureau, Hohhot (in Chinese)

Hill MC, Banta ER, Harbaugh AW, Anderman ER (2000) Modflow-2000, the U.S. Geological Survey modular ground-water model: user guide to observation, sensitivity, and parameter estimation processes, and three post-processing programs: U.S.Geological Survey Open-File Report 2000-184, 209 pp

Hillel D (2000) Salinity management for sustainable irrigation: integrating science, environment and economics. The World Bank, Washington DC, USA, 92 pp

Hinaman KC (1993) Use of a geographic information system to assemble input-data sets for a finite-difference model of ground-water flow. J Am Water Resour Assoc 29(3):401–405

Hollanders P, Schultz B, Wang SL, Cai LG (2005) Drainage and salinity assessment in the Huinong Canal Irrigation District, Ningxia. China. Irrig and Drain 54(2):155–173

IWC-IM (1999) Construction and rehabilitation planning project for water-saving in Hetao Irrigation District of the Yellow River basin. Inner Mongolia. Institute of Water Conservancy and Hydropower of Inner Mongolia, Hohhot (in Chinese)

Jarvis A, Reuter HI, Nelson A, Guevara E (2006) Hole-filled seamless SRTM data V3, International Centre for Tropical Agriculture (CIAT), available from http://srtm.csi.cgiar.org

Jha M, Chowdhury A, Chowdary V, Peiffer S (2007) Groundwater management and development by integrated remote sensing and geographic information systems: prospects and constraints. Water Resour Manage 21(2):427–467

Kolm KE (1996) Conceptualization and characterization of ground-water systems using Geographic Information Systems. Eng Geol 42:111–118

Legates D, McCabe G (1999) Evaluating the use of "goodness of fit" measures in hydrologic and hydroclimatic model validation. Water Resour Res 35(1):233–241

Li YN, Bai MJ, Pereira LS, Xu D, Cai LG (2004) Assessment of the seepage and performance of distribution system in Bojili Irrigation District. In: Huang GH, Pereira LS (Eds) Land and water management: decision tools and practices (proc. 7th inter-regional conf. environment and water, Beijing, Oct. 2004), vol 1. China Agriculture Press, Beijing, pp 1–10

Li HT, Kinzelbach W, Brunner P, Li WP, and Dong XG (2008) Topography representation methods for improving evaporation simulation in groundwater modelling. J Hydrol 356:199–208

Liu CM, Xia J (2004) Water problems and hydrological research in the Yellow River and the Huai and Hai River basins of China. Hydrol Process 18(12):2197–2210
Liu CM, Zheng HX (2004) Changes in components of the hydrological cycle in the Yellow River basin during the second half of the 20th century. Hydrol Process 18(12):2337–2345
Ma JZ, Wang XS, Edmunds WM (2005) The characteristics of ground-water resources and their changes under the impacts of human activity in the arid Northwest China—a case study of the Shiyang River Basin. J Arid Environ 61:277–295
MacDonald A (2001) Building a Geodatabase. ESRI, Redlands
McDonald MG, Harbaugh AW (1988) A modular three-dimensional finite-difference ground-water flow model. US Geological Survey, Techniques of Water-Resources Investigations of US Geological Survey. Book 6, CH.A1, Reston, Virginia
Mao XS, Jia JS, Liu CM, Hou ZM (2005) A simulation and prediction of agricultural irrigation on groundwater in well irrigation area of the piedmont of Mt. Taihang, North China. Hydrol Process 19(10):2071–2084
Moriasi DN, Arnold JG, Van Liew MW, Bingner RL, Harmel RD, Veith TL (2007) Model evaluation guidelines for systematic quantification of accuracy in watershed simulations. Trans ASABE 50(3):885–900
Mylopoulos N, Mylopoulos Y, Tolikas D, Veranis N (2007) Groundwater modelling and management in a complex lake–aquifer system. Water Resour Manage 21(2):69–494
Pereira LS, Cai LG, Musy A, Minhas PS (2003) Water saving in the Yellow River Basin: issues and decision support tools in irrigation. China Agricultural Press, Beijing
Pereira LS, Gonçalves JM, Dong B, Mao Z, Fang SX (2007) Assessing basin irrigation and scheduling strategies for saving irrigation water and controlling salinity in the Upper Yellow River Basin. China. Agric Water Manage 93(3):109–122
Pereira LS, Cordery I, Iacovides I (2009) Coping with water scarcity—addressing the challenges. Springer, Dordrecht
Ruan BQ, Han YP, Jiang RF (2008) Study on ecological water use in the Yellow River Irrigation District. In: Ruan BQ, Zhang RD, Li HA (Eds) Research on water balance and water consumption in Hetao Irrigation District. Science, Beijing, pp 99–123 (in Chinese)
San Juan C, Kolm KE (1996) Conceptualization, characterization and numerical modelling of the Jackson Hole alluvial aquifer using ARC/INFO and MODFLOW. Eng Geol 42:119–137
Shah N, Nachabe M, Ross M (2007) Extinction depth and evapotranspiration from ground water under selected land covers. Ground Water 45:329–338
Wang LP, Akae T (2004) Analysis of ground freezing process by unfrozen water content obtained from TDR data in Hetao Irrigation District of China. J Jpn Soc Soil Phys 98:11–19
Wang LP, Chen YX, Zeng GF (1993) Irrigation, drainage and salinization control in Hetao Irrigation District of Inner Mongolia. Water Resources and Hydraulic Power Publisher, Beijing (in Chinese)
Wang H, Yang Z, Saito Y, Liu JP, Sun X (2006) Interannual and seasonal variation of the Huanghe (Yellow River) water discharge over the past 50 years: connections to impacts from ENSO events and dams. Global Planet Change 50:212–225
Warrick AW (1988) Additional solutions for steady-state evaporation from a shallow water table. Soil Sci 146:63–66
Waterloo Hydrogeologic Inc. (2006) Visual MODFLOW pro user's manual. Waterloo Hydrogeologic Inc., Waterloo, Ontario, Canada
Wei ZM (2003) Study on crop–water relationship and availability of field irrigation water based on SWAP model simulation in arid area. PhD Dissertation, Inner Mongolia Agricultural University, Hohhot (in Chinese)
Wu JW, Vincent B, Yang JZ, Bouarfa S, Vidal A (2008) Remote sensing monitoring of changes in soil salinity: a case study in Inner Mongolia, China. Sensors 8(11):7035–7049
Xie CB, Cui YL, Lance JM (2003) Water supply systems: resource allocation, seepage and performance assessment. In: Pereira LS, Cai LG, Musy A, Minhas PS (Eds) Water savings in the Yellow River Basin: issues and decision support tools in irrigation. China Agricultural Press, Beijing, pp 46–64
Xu ZX, Takeuchi K, Ishidaira H, Zhang XW (2002) Sustainability analysis for Yellow River water resources using the system dynamics approach. Water Resour Manage 16:239–261
Xu X, Huang GH, Qu ZY (2009) Integrating MODFLOW and GIS technologies for assessing impacts of irrigation management and groundwater use in the Hetao Irrigation District, Yellow River basin. Sci China Ser E-Tech Sci 52(11):3257–3263

Xu X, Huang GH, Qu ZY, Pereira LS (2010) Assessing the groundwater dynamics and impacts of water saving in the Hetao Irrigation District, Yellow River basin. Agric Water Manage 98(2):301–313

Yang SQ (2005) Prediction and research of water-soil environment effect under light-saline water irrigation based on visual Modflow and SWAP coupling model in arid area. PhD Dissertation, Inner Mongolia Agricultural University, Hohhot (in Chinese)

Yu L (2006) The Huanghe (Yellow) River: recent changes and its countermeasures. Cont Shelf Res 26:2281–2298

Yu RH, Liu TX, Xu YP, Zhu C, Zhang Q, Qu ZY, Liu XM, Li CY (2010) Analysis of salinization dynamics by remote sensing in Hetao Irrigation District of North China. Agric Water Manage 97(12):1952–1960

Zhao FF, Xu ZX, Huang JX, Li JY (2008) Monotonic trend and abrupt changes for major climate variables in the headwater catchment of the Yellow River basin. Hydrol Process 22(23):4587–4599

Zhu Z, Giordano M, Cai X, Molden D, Hong S, Zhang H, Lian Y, Li H, Zhang X, Zhang X, Xue Y (2003) Yellow River comprehensive assessment: basin features and issues. IWMI, Colombo, Working Paper 57